

Optimum Control of Parabolic Trough Solar Fields with Partial Radiation^{*}

Sergio J. Navas^{*} Francisco R. Rubio^{**} Pedro Ollero^{***}

^{*} *Departamento de Ingeniería de Sistemas y Automática, Universidad de Sevilla, Spain (e-mail: snavas1@us.es).*

^{**} *Departamento de Ingeniería de Sistemas y Automática, Universidad de Sevilla, Spain (e-mail: rubio@us.es)*

^{***} *Departamento de Ingeniería Química y Ambiental, Universidad de Sevilla, Spain (e-mail: ollero@us.es)*

Abstract: This paper describes the main problems of operating parabolic trough solar fields during days with partial radiation. An optimal control strategy is proposed to solve these problems and it is assessed against a classical one, which uses a feedforward and a PI controller with a fixed set point of oil outlet temperature. Some simulations have been made using MATLAB to demonstrate that using the optimal control strategy better results can be achieved.

© 2017, IFAC (International Federation of Automatic Control) Hosting by Elsevier Ltd. All rights reserved.

Keywords: Solar, Control, Optimization, Parabolic Trough, Simulation, Partial Radiation

1. INTRODUCTION

The main technologies for converting solar energy into electricity are photovoltaic (PV) and concentrated solar thermal (CST). Parabolic trough, solar towers, Fresnel collector and solar dishes are the most used technologies for concentrating solar energy. This paper focus on parabolic trough solar fields, which consist of a collector field (Fig. 1), a power cycle and auxiliary elements such as pumps, pipes and valves. The solar collector field collects solar radiation and focuses it onto a tube in which a heat transfer fluid, usually synthetic oil, circulates. The oil is heated up and then used by the power cycle to produce electricity by means of a turbine.

The main goal of a parabolic trough solar field is to collect the maximum solar energy in order to produce as much electrical power as possible. Normally, this is achieved by keeping the outlet temperature of the field around the maximum allowable value, that is 400°C, due to oil degradation. However, in this paper, we will show that this way to operate the field does not produce the best results of electrical power generated. This problem has been studied before in Lippke (1995), where it was suggested that the optimum strategy is based on adapting the fluid outlet temperature to the incident solar radiation, keeping the constant the superheating temperature of the steam; it was also studied in Montes et al. (2009) where a constant outlet temperature was used (393°C). Finally, a more recent study was carried out in Camacho and Gallego (2013) where it was proposed to change the outlet temperature set point according to the value of the solar radiation.

On the other hand, using a PI with a feedforward controller that manipulates the oil flow to keep constant the outlet temperature of the field, like in Camacho et al. (1997)-Camacho et al. (2012)-Carmona (1985), while a cloud is passing through the field may provoke temperature peaks in some loops. This situation is due to the fact that when the cloud passes the controller will decrease the oil flow in order to keep the outlet temperature constant, however, in the loops that are not covered by the cloud, the solar radiation is not reduced, so that their temperature will be increased above the security limit. If this situation happens the collectors are programmed to get out of focus to prevent oil degradation, but that would involve a loss of energy and it is not considered in this paper as a possible solution.

In this paper the effect of the solar radiation on the outlet temperature was studied with a complete power cycle model (Fig. 2) reduced to a correlation that relates the electrical power generated by the condensation turbine with the mass flow and outlet temperature of the oil. In Camacho and Gallego (2013) it is used a similar approach but they use a correlation that only depends on the outlet temperature, that implies efficiency results higher than the ones found in the literature Lippke (1995); in addition the simulations made in this paper were carried out taking into account a model of the entire field, not assuming that the behavior of one loop is the same than the other ones. Therefore, the authors propose that using an optimal controller with constraints can prevent the appearance of temperature peaks and also maximize the electrical power generated by the field depending on the value of solar radiation.

The paper is organized as follows: Section 2 describes the models of the solar field, passing clouds and power cycle used for simulation purposes. Section III describes both

^{*} This work was supported by the projects DPI2013-44135-R and DPI2015-70973-R granted by the Spanish Ministry of Science and Innovation.

control strategies tested: the feedforward with a PI control and the optimum control. Section IV shows the results obtained by simulations made in MATLAB. Finally, the paper draws to a close with some concluding remarks.



Fig. 1. ACUREX distributed solar collector field

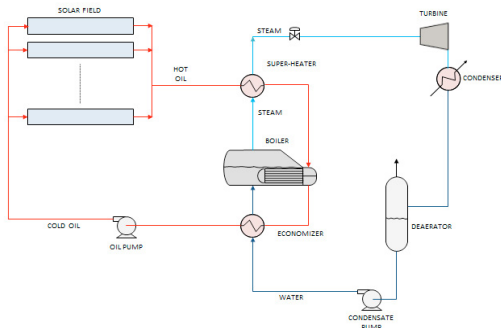


Fig. 2. Diagram of the solar field connected with the power cycle

2. SYSTEM MODELING

The model of each of the parts which have been used to simulate the operation of a solar field during the days with partial covering is presented. These parts are: the solar collector field, the passage of the clouds and the power cycle.

2.1 Solar Collector Field Model

In this subsection, the mathematical model of a parabolic trough solar field is presented. This model is the same used in Navas et al. (2016) which is at the same time a slight modification of the model proposed by Camacho et al. (1997)-Camacho et al. (2012)-Carmona (1985) for the ACUREX field (Fig. 1). Basically, this model can be used to simulate parabolic trough solar fields by selecting parameters like the number of active (the parts where the solar radiation reaches the tube) and passive (joints and other parts not reached by concentrated solar radiation) zones, length of each zone, or collector aperture. The solar field simulated in this paper is supposed to be on the site of the Escuela Superior de Ingeniería de Sevilla. It is composed of 24 loops and has dimensions of $144 \times 240 \text{ m}^2$. Each loop is modeled by the following system of partial

differential equations describing the energy balance:

Active zones

$$\rho_m C_m A_m \frac{\partial T_m}{\partial t} = I n_0 G - H_l G (T_m - T_a) - L H_t (T_m - T_f) \quad (1)$$

Fluid element

$$\rho_f C_f A_f \frac{\partial T_f}{\partial t} + \rho_f C_f \dot{q} \frac{\partial T_f}{\partial x} = L H_t (T_m - T_f) \quad (2)$$

Passive zones

$$\rho_m C_m A_m \frac{\partial T_m}{\partial t} = -H_p (T_m - T_a) - L H_t (T_m - T_f) \quad (3)$$

where the sub-index m refers to metal and f refers to the fluid. The model parameters and their units are shown in table 1.

Table 1. Solar field model parameters description

Symbol	Description	Units
t	Time	s
x	Space	m
ρ	Density	Kg/m^3
C	Specific heat capacity	$\text{J}/(\text{K kg})$
A	Cross sectional area	m^2
T	Temperature	$^\circ\text{C}$
\dot{q}	Oil flow rate	m^3/s
I	Solar radiation	W/m^2
n_0	Optical efficiency	Unit-less
G	Collector aperture	M
T_a	Ambient Temperature	$^\circ\text{C}$
H_l	Global coefficient of thermal losses for active zones	$\text{W}/(\text{m}^2 \text{ } ^\circ\text{C})$
H_t	Coefficient of heat transmission metal-fluid	$\text{W}/(\text{m}^2 \text{ } ^\circ\text{C})$
H_p	Global coefficient of thermal losses for passive zones	$\text{W}/(\text{m}^2 \text{ } ^\circ\text{C})$
L	Length of pipe line	m

The density ρ , specific heat C and coefficient of thermal loss H_l depend on fluid temperature. The coefficient of heat transmission H_t depends on temperature and oil flow. The incident solar radiation I depends on hourly angle, solar hour, declination, Julianne day, local latitude and collector dimensions Camacho et al. (1997)-Camacho et al. (2012)-Carmona (1985). In order to solve this system of partial differential equations, a two stage finite difference equation has been programmed, considering each segment of 1 m for the passive zones and of 3 m for the active zones and solving (1)-(2)-(3).

2.2 Modeling of the Passing Clouds

The modeling of the passing clouds is necessary to know how the radiation of the sun is distributed throughout the field. This can be achieved creating a matrix which represents the whole field extension. Each element of the matrix is assigned the value of the incident solar radiation

on that section at each time. The solar field has dimensions of $144 \times 240 \text{ m}^2$, so if we divide the matrix in elements of 3×3 meters we need a 48×80 matrix. The matrix is then put over the field in such a way that each element contains a fraction of an active or passive element. Fig.3 shows the fraction of the whole matrix that covers one loop of a generic field.

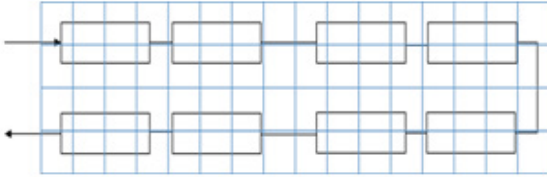


Fig. 3. Example of a fraction of the matrix over one loop of the field

The value of the radiation in each element of the matrix depends on the following parameters:

- The global incident solar radiation on the field.
- The direction of the route followed by the passing cloud (the angle formed by this direction and the direction followed by the thermal fluid, the parallel being 0).
- The velocity of the passing cloud (determined by the number of elements of the matrix supposed to be traveled by the cloud every 39 seconds, which is the sample time of the field).
- The size of the cloud (a rectangular form is supposed, defined by the rows and columns that it covers).
- The attenuation factor, which is the value that multiplies the radiation in the zones where the cloud is present. This value varies between 0 and 1 depending on the radiation which the cloud allows to arrive to the field, being 0 the case in which no radiation arrives to the field and 1 the case in which all the radiation arrives to it.

Once these values are set, the program calculates for each collector the mean value of radiation of every element of the matrix related with it. This mean value is assigned to the variable I of (1).

2.3 Power Cycle Model

The power cycle model used in this paper (Fig. 2) consists of an economizer, a boiler and a super-heater followed by a turbine. The oil flow heated by the solar radiation concentrated by field collectors is firstly introduced into the super-heated where a steam stream is heated. Afterward, the oil is used to produce saturated steam in the boiler, which operates at a floating pressure. Finally the oil is sent to the economizer to preheat the water stream before being boiled. The super-heated steam is used to produce electrical power in a condensation turbine.

This model was simulated using the software Engineering Equation Solver and then correlated with simulation results to get equations (4) and (5) in order to calculate the electrical power generated and the oil temperature

returning to the field respectively. This simplification was necessary to reduce the simulation time and the error is around 1%. In addition the dynamic of the cycle was assumed to be like a first order model with a time constant of 100 seconds.

$$W = 8.23e^3 - 49.96m_{oil} - 2.70m_{oil}^2 - 47.15T_{out} + 6.75e^{-2}T_{out}^2 + 5.38e^{-1}m_{oil}T_{out} \quad (4)$$

$$T_{in} = 3.40e^2 + 1.78m_{oil} - 1.55e^{-1}m_{oil}^2 - T_{out} + 1.07e^{-3}T_{out}^2 + 2.17e^{-2}m_{oil}T_{out} \quad (5)$$

The net electrical power produced by the field is the result of subtracting the power consumed by the pump to the power generated by the turbine. Therefore, to calculate the consumption of the pump we used the Darcy equations. Firstly, the Reynolds number and the Barr's friction coefficient are computed by (6) and (7) respectively:

$$Re = \frac{\rho_f q d}{A_f \mu} \quad (6)$$

$$f = 0.25 \frac{1}{\log_{10}(\epsilon_r/3.7d + 5.74/Re^{0.9})^2} \quad (7)$$

where μ is the dynamic viscosity and ϵ_r is the relative rugosity. The Darcy equation for computing the pressure drop is given by (8):

$$hpl = 9806.65 \frac{8fLq^2}{g\pi^2 d^5} (Pa) \quad (8)$$

where L is the loop length and d is the pipe diameter. The power consumption depends on the pump efficiency, oil flow and the pressure drop pd (9).

$$W_{pump} = \frac{qhpl}{\eta_{pump}} (W) \quad (9)$$

Finally, the net electrical power is calculated by (10).

$$W_{net} = W - \frac{W_{pump}}{1000} (kW) \quad (10)$$

3. CONTROL STRATEGIES

In this section two control strategies are presented. The feedforward with PI control strategy is the traditional one used in solar fields to keep constant the oil outlet temperature, whereas the Optimal control strategy is a new one proposed by the authors in order to maximize the electrical power generated and prevent the appearance of temperature peaks.

3.1 Feedforward with PI Control

This control strategy consists of controlling the outlet temperature of the field by manipulating the total flow of the oil. This total flow is equally distributed among the loops. The control scheme can be seen in Fig. 4, where a series feedforward compensation is used.

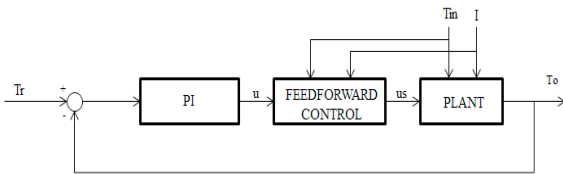


Fig. 4. Series feedforward controller

The feedforward controller provides compensation for variations in I and T_{in} calculating the desired flow of oil u_s using (11), where T_0 is the outlet temperature to be maintained, Pc_p is a term that accounts for the product and quotient of characteristic magnitudes (areas, thermal capacities, etc.), S is the effective surface, H_l is the global thermal losses coefficient, and T_m is the mean inlet-outlet temperature. Equation (11) comes from the concentrated parameters model of the field Camacho et al. (1997)-Camacho et al. (2012)-Carmona (1985) considering steady state conditions. This equation can be approximated by (12), where u is the output of a PI controller ($K_c = 1.09$, $\tau_i = 150.28$ s) placed before the feedforward controller in order to maintain the required steady state outlet temperature T_0 due to the fact that exact compensation cannot be achieved with it.

$$(T_0 - T_{in})u_s = \frac{1}{Pc_p}(n_0SI - H_l(T_m - T_a)) \quad (11)$$

$$u_s = \frac{3.15I - 0.204(u - 64.16) - 75.87}{u - T_{in}} \quad (12)$$

The radiation I used in (12) is the global incident solar radiation on the field which is calculated as the mean value of all elements of the matrix, and the variable T_{in} is the inlet temperature of the thermal fluid, calculated by (5). The constants that appear in the equation have been determined experimentally.

3.2 Optimal Control

This control strategy is based on using an MPC controller, which uses models of the field and the power cycle, so that the controller could calculate the optimum value of oil outlet temperature which maximizes the electrical power generated, taking into account temperature and oil flow constraints. The control scheme can be seen in Fig.5. The dynamic optimization procedure may be expressed as the following algorithm:

- All the variables needed by the field model are measured.
- A simplified solar collector field model (1)-(2), which assumes that the pipe is only divided in 6 parts of 80 meters instead of the divisions of 1 meter for passive zones and 3 meters for the active zones in the model used for simulating the solar field, is used to calculate the outlet oil temperature of the field. The oil flow is the independent variable used by the optimizer.
- With the calculated values of oil outlet temperature and mass oil flow, equations (4) and (5) are used to know the electrical power generated by the turbine and the inlet oil temperature.

- Finally, with equations (6), (7), (8), (9) and (10) the net electrical power is calculated.

Therefore, the MPC has to maximize the value of net electrical power subject to restrictions in oil temperature ($T \leq 400^\circ\text{C}$) and oil flow ($0.000133 \text{ m}^3/\text{s} \leq q \leq 0.00158 \text{ m}^3/\text{s}$) for each loop. The prediction and control horizons are equal to one, however, in future works, it is planned to increase these horizons incorporating predictions of the passing clouds. The optimization is carried out for each integration step by the function *fmincon* in MATLAB. The optimum value of oil flow would be then sent as the new set point of the flow controller, which manipulates the variable frequency drive, but in this simulation we are assuming that the flow is instantly changed.

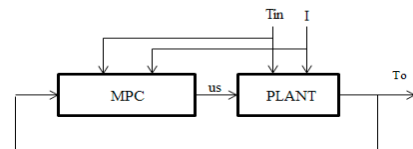


Fig. 5. MPC controller

4. SIMULATION RESULTS

This section shows the results obtained by simulations of both strategies explained in Section 3. These simulations have been carried out with the solar radiation curve shown in (Fig. 6) and using the models described in section 2. If we compared the feedforward with PI strategy with a fixed set point of 393°C against the optimal one, we can see that the feedforward with PI strategy presents the problem of temperature peaks in some loops (Fig. 7) whereas in the optimal strategy this situation does not happen (Fig. 8). The oscillations observed in Fig. 7 are due to use of a static feedforward with unmodelled dynamics; a problem that does not occur when the optimal controller is used (Fig. 8). In terms of electrical power (Fig. 9), it seems that during the central part of the day the feedforward strategy produces more than the optimal one, but at the cost of having temperature peaks. However, during the last part of the day, when the value of the incident solar radiation is low, the optimal strategy produces much more electrical power. Considering the entire operating day, the improvement achieved by the optimal strategy is around 2.15%.

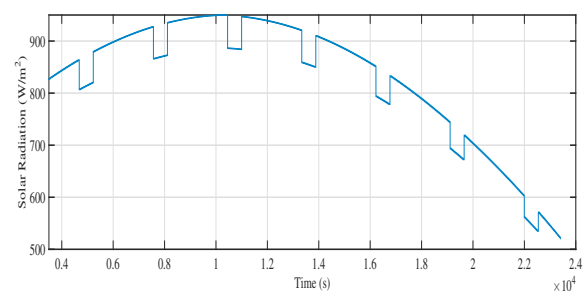


Fig. 6. Incident solar radiation

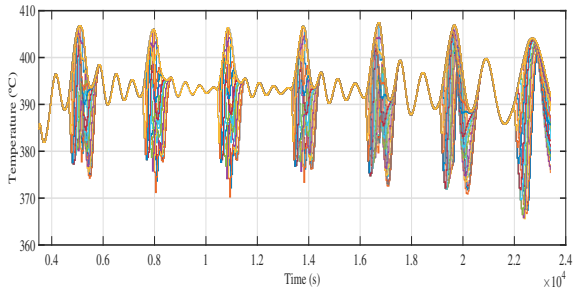


Fig. 7. Oil outlet temperature of the loops with a feedforward controller and a set point of 393°C

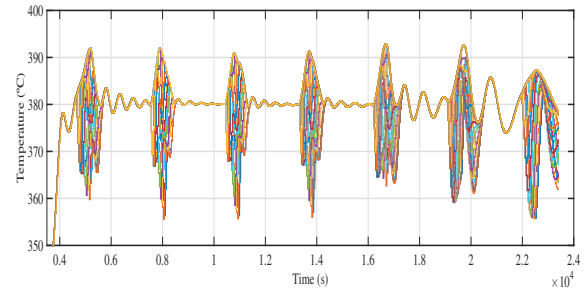


Fig. 10. Oil outlet temperature of the loops with a feedforward controller and a set point of 380°C

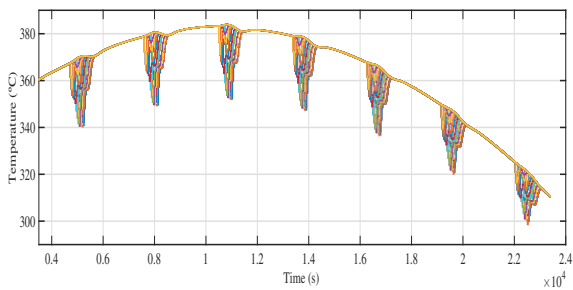


Fig. 8. Oil outlet temperature of the loops with an optimal controller

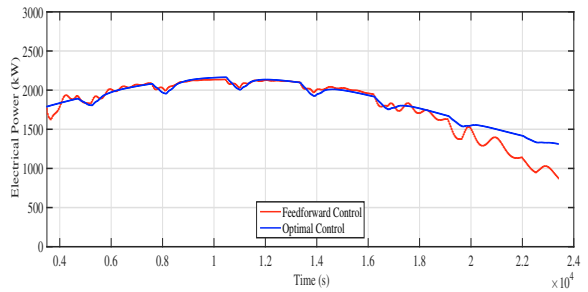


Fig. 11. Electrical power generated by the optimal strategy and the feedforward strategy with a set point of 380°C

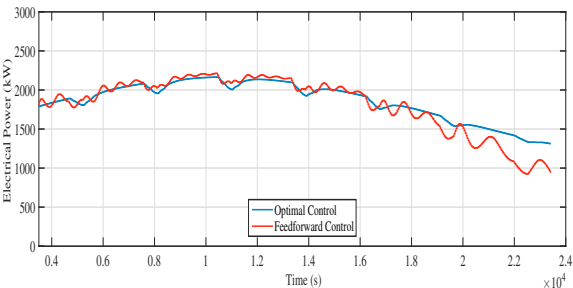


Fig. 9. Electrical power generated by the optimal strategy and the feedforward strategy with a set point of 393°C

After seeing that with the feedforward with PI strategy with a set point of 393°C we could not avoid the problem of the appearance of temperature peaks, we tested the same strategy but with a lower set point equal to 380°C. Figure 10 shows that with this set point the temperature peaks do not appear, however, in terms of electrical power this new set point has worse results than the previous one (Fig. 11). Specifically, in this case the improvement achieved when compared with the optimal strategy is around 2.95%.

5. CONCLUSION

The main conclusion of this paper is, that to operate the field during a day with partial radiation at a constant oil outlet temperature is not the optimum way to do it and also can lead to the temperature peaks problem. Using the feedforward with PI strategy the only way to avoid this problem is to lower the oil outlet temperature set point, but in doing so, it also reduces the total amount of electrical power generated. For that reason the authors propose the use of the optimal strategy, which can prevent the temperature peaks problem and also maximizes the electrical power production, not only when there are passing clouds, but also when the value of the incident solar radiation is low.

ACKNOWLEDGEMENTS

The authors wish to thank Professor João Lemos for his valuable comments and suggestions.

REFERENCES

- Abutayeh, M., Alazzam, A. and El-Khasawneh, B. (2014) Balancing heat transfer fluid flow in solar fields. *Solar Energy*, 105, 381-389.
- Barão, M., Lemos, J. and Silva, R. (2002). Reduced complexity adaptive nonlinear control of a distributed collector solar field. *Journal of Process Control*, 12-1, 131-141.
- Camacho, E. F., Berenguel, M. and Rubio, F. R. (1997). *Advanced control of solar plants*. Springer-Verlag, London.

- Camacho, E. F., Rubio, F. R., Berenguel, M. and Valenzuela, L. (2007). A survey on control schemes for distributed solar collector fields. Part I: Modeling and basic control approaches. *Solar Energy*, 81-10, 1240-1251.
- Camacho, E. F., Rubio, F. R., Berenguel, M. and Valenzuela, L. (2007). A survey on control schemes for distributed solar collector fields. Part II: Advanced control approaches. *Solar Energy*, 81-10, 1252-1272.
- Camacho, E. F., Berenguel, M., Rubio, F. R. and Martínez, D. (2012). *Control of solar energy systems*. Springer-Verlag, London.
- Camacho, E. F. and Gallego, A. (2013). Optimal operation in solar trough plants: A case study. *Solar Energy*, 95, 106-117.
- Carmona, R. (1985). *Análisis, modelado y control de un campo de colectores solares distribuidos con sistema de seguimiento en eje*. Ph.D. Thesis.
- Cirre, C., Berenguel, M., Valenzuela, L. and Camacho, E. F. (2007). Feedback linearization control for a distributed solar collector field. *Control Engineering Practice*, 15-12, 1533-1544.
- Cirre, C., Berenguel, M., Valenzuela, L. and Klempous, R. (2009). Reference governor optimization and control of a distributed solar collector field. *European Journal of Operational Research*, 193, 709-717.
- Colmenar-Santos, A., Munuera-Prez, F., Tawfik, M. and Castro-Gil, M. (2014). A simple method for studying the effect of scattering of the performance parameters of parabolic trough collectors on the control of a solar field. *Solar Energy*, 99, 215-230.
- Gallego, A. and Camacho, E. F. (2012). Estimation of effective solar irradiation using an unscented kalman filter in a parabolic-trough field. *Solar Energy*, 86-12, 3512-3518.
- Lima, D., Normey-Rico, J. and Santos, T. (2016). Temperature control in a solar collector field using filtered dynamic matrix control. *ISA Transactions*, 62, 39-49.
- Lippke, F. (1995). Simulation of the part-load behavior of a 30 MWe SEGS plant. Report No. SAND95-1293, SNL, Albuquerque, NM, USA.
- Montes, M., Abánades, A., Martínez-Val, J. and Valdés, M. (2009). Solar multiple optimization for a solar-only thermal power plant, using oil as heat transfer fluid in the parabolic trough collectors. *Solar Energy*, 83-12, 2165-2176.
- Navas, S. J., Rubio, F. R., Ollero, P. and Ortega, M. G. (2016). Modeling and simulation of parabolic trough solar fields with partial radiation. *XV European Control Conference*, 31-36.
- Price, H., Lufert, E., Kearney, D., Zarza, E., Cohen, G., Gee, R. and Mahoney, R. (2002). Advances in parabolic trough solar power technology. *Solar Energy*, 124-2, 109-125.
- Rubio, F. R., Camacho, E. F. and Berenguel, M. (2014). Control de campos de colectores solares. *Ibero-American Journal of Industrial Automation and Informatics (RIAI)*, 3-4, 26-45.
- Shinskey, F. (1978). *Energy conservation through control*. Academic Press.
- Smith, R. (2005). *Chemical process design and integration*. Wiley.